

Supporting Information

ARCHE-NOAH: NMR Supersequence with Five Different CEST Experiments for Studying Protein Conformational Dynamics

Rodrigo Cabrera Allpas,^a Alexandar L. Hansen,^b Rafael Brüschweiler^{a,b,c*}

¹Department of Chemistry and Biochemistry, The Ohio State University, Columbus, Ohio 43210, U.S.A.

²Campus Chemical Instrument Center, The Ohio State University, Columbus, Ohio 43210, U.S.A.

³Department of Biological Chemistry and Pharmacology, The Ohio State University, Columbus, Ohio 43210, U.S.A.

Materials and Methods

The ARCHE-NOAH supersequence was tested on 1mM of a uniformly ^{15}N -, ^{13}C -labeled Im7 sample in 97%/3% $\text{H}_2\text{O}/\text{D}_2\text{O}$ and 50mM sodium phosphate, pH 7.0. All NMR experiments were performed on an 850 MHz Bruker Ascend magnet equipped with an Avance III HD console and a triple resonance inverse cryoprobe. In total, six experiments were performed: ^{15}N -CEST, ^{13}CO -CEST, $^{13}\text{C}_\alpha$ -CEST, ^{13}C -aromatic-CEST, and ^{13}C -methyl-CEST experiments with ^1H -start magnetization and the ARCHE-NOAH supersequence with all five modules (**Fig. 1**). All experiments were recorded with $2\text{k} \times 160$ complex points along the F3 and F2 dimensions, respectively, together with 68 CEST offset saturation frequencies in the pseudo 3rd dimension F1. For the ARCHE-NOAH sequence, this is accomplished in Topspin by setting the F1 parameter to $5 \times 68 = 340$. Four transients per FID were obtained with an acquisition time of 75 ms and 180 dummy scans. The recovery delay $d1$ used for all sequences was 2 seconds. The proton spectral width was 16 ppm for all experiments and the nitrogen spectral width was 35 ppm for the ^{15}N -CEST and ARCHE-NOAH. The carbon spectral width was 14, 60, 40, and 35 ppm for the standalone and the ARCHE-NOAH ^{13}CO -CEST, ^{13}C -aromatic-CEST, ^{13}C -aromatic-CEST, $^{13}\text{C}_\alpha$ -CEST, and ^{13}C -methyl-CEST experiments, respectively. The ^1H carrier position was kept at the water resonance (4.7 ppm) and the carrier position for ^{15}N was 118 ppm. The carrier position for ^{13}C was 100, 175, 125, 58, and 70 ppm for the standalone and the ARCHE-NOAH ^{15}N -CEST, ^{13}CO -CEST, $^{13}\text{C}_\alpha$ -CEST, ^{13}C -aromatic-CEST, and ^{13}C -methyl-CEST experiments, respectively. For the ^{13}C -aromatic-CEST module, the carbon carrier position changes briefly to 135 ppm prior to selective carbon decoupling to ensure that all aromatic carbons are decoupled while not perturbing the aliphatic carbon region. The B_1 field for the standalone and the ARCHE-NOAH sequences were 25, 50, 50, 40, 40 Hz for ^{15}N -CEST, ^{13}CO -CEST, $^{13}\text{C}_\alpha$ -CEST, ^{13}C -aromatic-CEST, and ^{13}C -methyl-CEST experiments, respectively, with a T_{ex} of 500, 200, 200, 300 and 300 ms.

The ARCHE-NOAH ^{13}C -start modules used Q5 and Q3 band selective pulses to excite or invert the magnetization of interest without perturbing other types of ^{13}C spins.¹ Other selective pulses used are the Reburp and Iburp2 pulses for aliphatic and carbonyl inversion in the $^{13}\text{C}_\alpha$ -CEST and ^{13}C -methyl-CEST both for the standalone experiments and ARCHE-NOAH.²

All spectra were initially processed in Topspin 3.6.2. The Bruker AU program “split” was used to separately obtain the resulting spectra from each type of CEST experiment and an AU program written in-house was used to fix the carbon spectral width and carrier position after data splitting. Further processing was done using NMRPipe with scripts written in-house for the processing of pseudo-3D experiments. Peak fitting was done in NMRPipe and the resulting CEST profiles were

obtained and fitted using the ChemEx software (<http://www.github.com/gbouvignies/chemex>) for a 2-site exchange process. For the signal-to-noise ratio calculation, the noise level was determined using median absolute deviation (MAD) in a region of the spectra free of resonances (consisting of ~35k points) using MATLAB (Version R2021b, The Mathworks, Inc, Natick, MA).

Comparison of standalone spectra vs ARCHE-NOAH

The quality of the spectra of the ^1H -start standalone ^{15}N -CEST, ^{13}CO -CEST, ^{13}C -aromatic-CEST, $^{13}\text{C}_\alpha$ -CEST, and ^{13}C -methyl-CEST is compared with each ARCHE-NOAH module after splitting and processing of the data (**Figure S1 - S5**). As mentioned in the methods section, each sequence was acquired with the same NMR parameters, except for the selective pulses used in the ARCHE-NOAH pulse sequence.

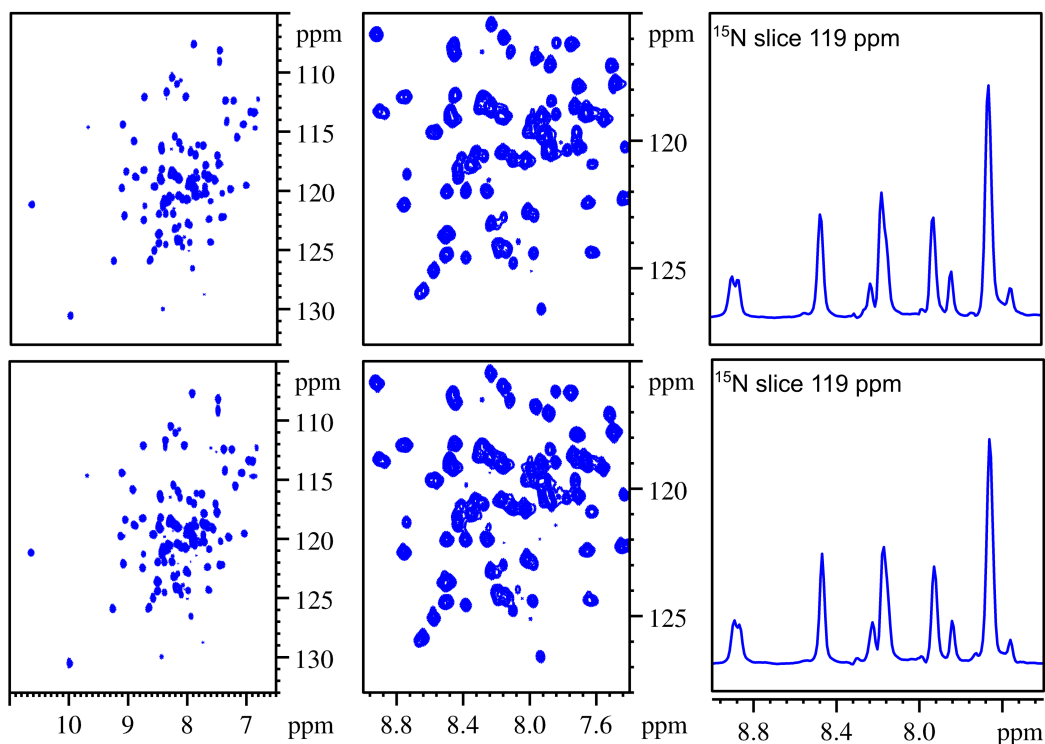


Figure S1. Comparison between standalone ^{15}N -CEST (top row) vs ^{15}N -CEST module of the ARCHE-NOAH (bottom row). The left column represents the entire reference spectra of each experiment (^1H : 11.0 - 6.5 ppm, ^{15}N : 133.0 - 105.0 ppm), the middle column shows the same expanded region (^1H : 9.0 - 7.4 ppm, ^{15}N : 128.0 - 115.0 ppm) of the two experiments, and the right column shows 1D slices taken at 119 ppm (^{15}N) demonstrating good agreement between these experiments.

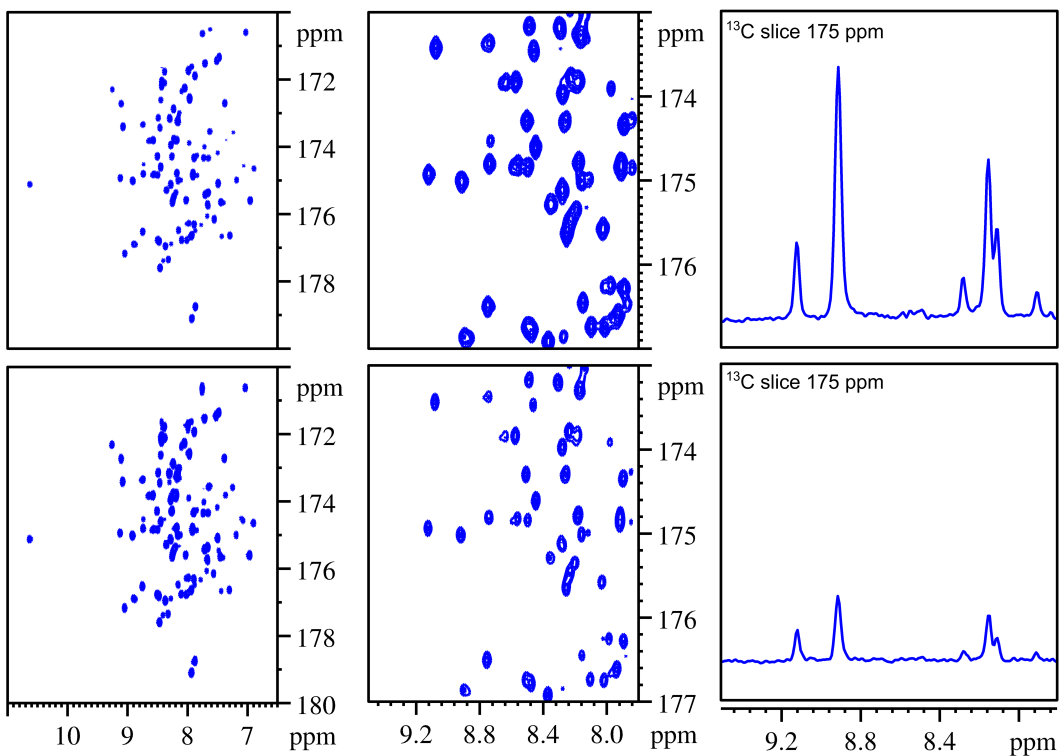


Figure S2. Comparison between standalone ^{13}C O-CEST (top row) vs ^{13}C O-CEST module of the ARCHE-NOAH (bottom row). The left column represents the entire reference spectra of each experiment (^1H : 11.0 - 6.5 ppm, ^{13}C : 180.0 - 170.0 ppm), the middle column shows the same expanded region (^1H : 9.5 - 7.8 ppm, ^{13}C : 177.0 - 173.0 ppm) of the two experiments, and the right column shows 1D slices taken at 175 ppm (^{13}C) demonstrating good agreement between these experiments.

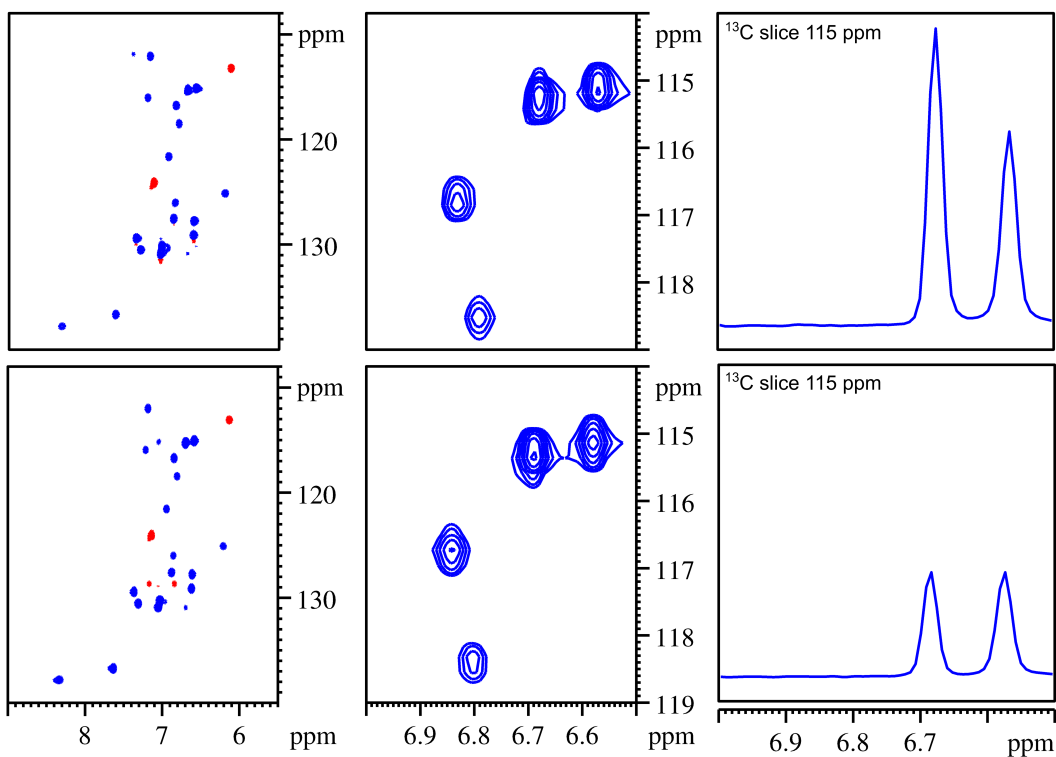


Figure S3. Comparison between standalone ^{13}C -aromatic-CEST (top row) vs ^{13}C -aromatic-CEST module of the ARCHE-NOAH (bottom row). Red contours indicate peaks with negative amplitude. The left column represents the entire reference spectra of each experiment (^1H : 9.0 - 5.5 ppm, ^{13}C : 140.0 - 108.0 ppm), the middle column shows the same expanded region (^1H : 7.0 - 6.5 ppm, ^{13}C : 119.0 - 114.0 ppm) of the two experiments, and the right column shows 1D slices taken at 115 ppm (^{13}C) demonstrating good agreement between these experiments.

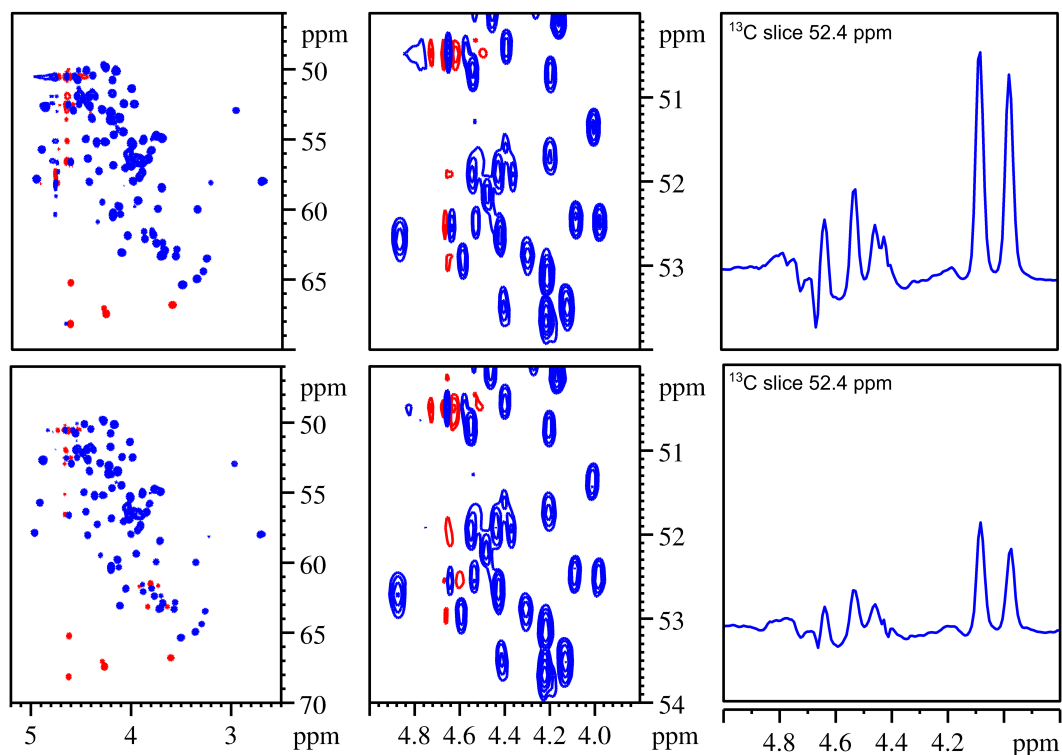


Figure S4. Comparison between standalone $^{13}\text{C}_\alpha$ -CEST (top row) vs $^{13}\text{C}_\alpha$ -CEST module of the ARCHE-NOAH (bottom row). Red contours indicate peaks with negative amplitude. The left column represents the entire reference spectra of each experiment (^1H : 5.2 - 2.5 ppm, ^{13}C : 70.0 - 46.0 ppm), the middle column shows the same expanded region (^1H : 5.0 - 3.8 ppm, ^{13}C : 54.0 - 50.0 ppm) of the two experiments, and the right column shows 1D slices taken at 52.4 ppm (^{13}C) demonstrating good agreement between these experiments.

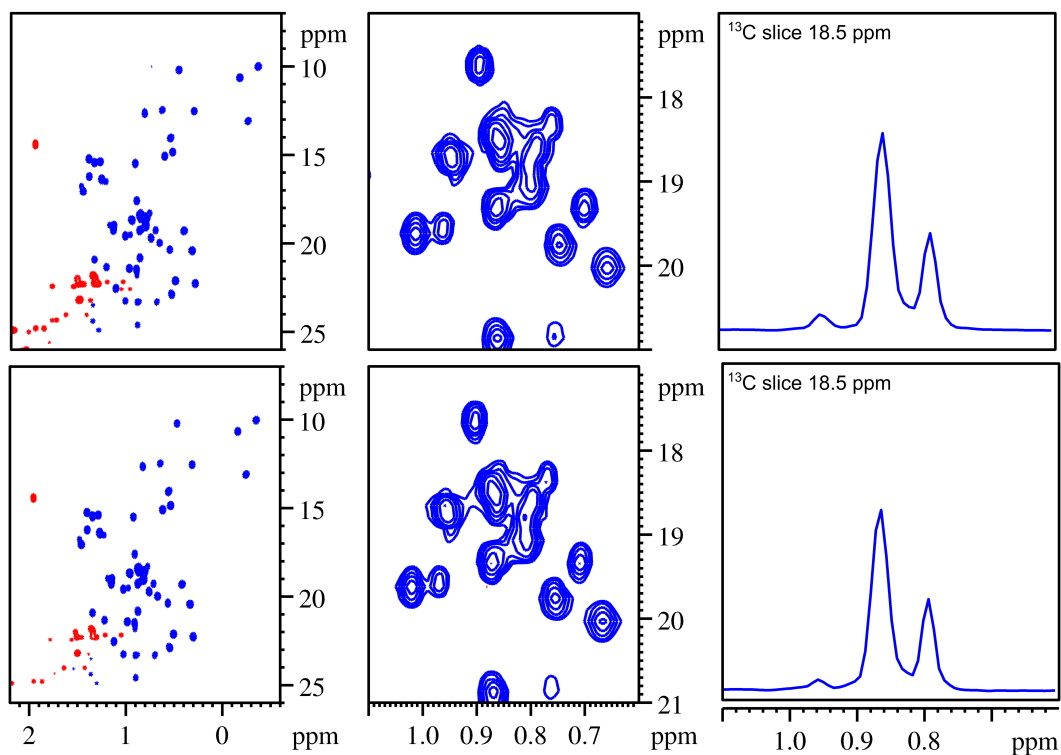


Figure S5. Comparison between standalone ^{13}C -methyl-CEST (top row) vs ARCHE-NOAH (bottom row). Red contours indicate peaks with negative amplitude. The left column represents the entire reference spectra of each experiment (^1H : 2.2 - -0.6 ppm, ^{13}C : 26.0 - 7.0 ppm), the middle column shows the same expanded region (^1H : 1.1 - 0.6 ppm, ^{13}C : 21.0 - 17.0 ppm) of the two experiments, and the right column shows 1D slices taken at 18.5 ppm (^{13}C) demonstrating good agreement between these experiments.

ARCHE-NOAH selective pulses

ARCHE-NOAH employs multiple selective pulses across each respective module to select a specific carbon magnetization pool. The pulses shown in **Table S1** are all available in the Topspin pulse library.

Table S1. Parameters of the selective pulses employed in the ARCHE-NOAH supersequence.

ARCHE-NOAH module	Selective pulse	Pulse width (us)	Carrier position (ppm)	$\gamma B_{1,max}$ (Hz)
^{13}CO -CEST module	Q5*	650	175	7055.87
	Q3	450	175	7335.25
	Q3	550	58	6001.57
^{13}C -aromatic-CEST	Q5*	350	135	13103.76
	Q3	260	135	12695.63
	Cawurst-8	1000	125	2803.26
$^{13}\text{C}_\alpha$ -CEST	Q5*	900	58	5095.91
	Q3	600	17	5501.44
	lburp2*	244	147.5	20361.87
	Reburp	259	40	24188.67
	Q3	550	58	6001.57
	Cawurst-8	1400	58	5421.13
^{13}C -methyl-CEST	Reburp	259	44	24188.67
	Reburp	905	18	6922.50
	lburp2*	244	147.5	20361.87

* For these pulses, a time reverse version (e.g. Q5tr) was also employed when required.

In our CEST sequences, neither sensitivity loss nor artifacts were observed when using selective pulses versus broadband pulses. One minor complication that was dealt with is that the carrier position used by the selective pulses of the aromatic-CEST modules needed to be at a lower field than the standalone experiment (135 ppm vs 125 ppm). This is because of carbons such as C_γ and C_ζ in tyrosine residues that need to be excited and inverted to suppress carbon-carbon couplings. These carbons are not visible in a HSQC spectrum since they do not have a proton

attached. Hence, the user needs to choose a sufficiently broad excitation bandwidth to cover them (i.e. up to 160 - 170 ppm). Further instructions on setting up these selective pulses are in the pulse program, which can be found at <https://github.com/RCabreraAlpas>. The Wavemaker app in Topspin can be used to create these shapes automatically, along with their parameters.

References

1. L. Emsley and G. Bodenhausen, *J. Magn. Reson.* 1969, 1992, 97, 135–148.
2. H. Geen and R. Freeman, *J. Magn. Reson.* 1969, 1991, 93, 93–141.